Versatile and potent insecticide scavengers based on locust cell membrane-adapted mesoporous silicon microparticles to protect managed pollinators

Jing Chen

jingchen3236@njucm.edu.cn

Nanjing University of Chinese Medicine https://orcid.org/0000-0002-2681-0349

Zuliang Huang

Soochow University

Jiakun Guo

Soochow University

Suhui Lv

Nanjing University of Chinese Medicine

Jie Gui

Nanjing University of Chinese Medicine

Zhiyuan Zhong Zhiyuan Zhong

Soochow University

Chao Deng

Soochow University

Article

Keywords:

Posted Date: September 11th, 2024

DOI: https://doi.org/10.21203/rs.3.rs-4688813/v1

Additional Declarations: There is **NO** Competing Interest.

Abstract

Sustainable agriculture highly relies on pollinators which affect the production and diversity of around 75% of foodcrops worldwide. However, the population and fitness of pollinators are showing sharp declining trends for years. Exposure to insecticides especially during crop pollination together with lacking effective management method has been reported as a dominant factor. Here, we have developed versatile and potent insecticide scavengers based on locust cell membrane and tannic acid (TA)-coated mesoporous silicon microparticles (MTSM) to prevent pollinators from a broad-spectrum insecticides including organophosphorus, pyrethroids, and neonicotinoids. Leveraging the π-π stacking with TA and specific binding by the acetylcholinesterases, nicotine receptors of acetylcholine, or voltage-gated sodium channels on locust cell membrane, MTSM presented enormously high removal efficiency of various insecticides while minimum nonspecific clearance of favorable enzymes mainly exsisting in gastrointestinal system of bees. Notably, MTSM exhibited over 12 h residency in gastrointestinal tract of bumblebees to facilitate insecticide scanvenging, and could be almost entirly excreted from bees within 48 h, causing no death of bees even at a high concentration of 50 mg/mL. In microcolonies of bumblebee fed with insecticide-contaminated impatien pollen patties, MTSM revealed dose-dependent detoxicification capacity towards organophosphorus and neonicotinoids insecticides. In sharp constrast to complete death of bumblebees fed with triazophos at a dose of 98 ng/bee within 5 days, the survival rate of bumblebees was significantly elevated to 75% and 90% by MTSM at doses of 1.0 and 20 mg/mL within 10 days, respectively. Overall, MTSM combining the merits of good safety, facile construction, and efficient and broad-spectrum detoxification presents versatile and potent scavengers to protect managed pollinators from multiclass insecticides.

Highlights

1. Versatile and potent insecticide scavengers have been facilely constructed through surface decoration of mesoporous silicon microparticles with tannic acid (TA) and locust cell membrane sequentially (MTSM);
2. Leveraging π-π stacking with TA and specific membrane binding, MTSM presents enormously high removal efficiency of a broad-spectrum insecticides including organophosphates, pyrethroids, and neonicotinoids, while minimum nonspecific clearance of favorable enzymes existing in the gastrointestinal system of pollinators;
3. MTSM can be almost entirely excreted from bees within 48 h and causes no death of bees even at a high concentration of 50 mg/mL, signifying the excellent safety;
4. With over 12 h residency in gastrointestinal tract of bumblebees, MTSM exhibites extensive insecticides scavenging, affording dose-dependent detoxification efficacy towards organophosphates and neonicotinoids insecticides as well as significantly elevated survival rate up to 90%.

Introduction

Pollinators play a vital role in maintaining ecosystem resilience and supporting global agriculture production with approximately $351 billion contribution annually [1–3]. However, the overuse of insecticides (600 000 tons/year, globally) for pest control induces unintended survival stress towards pollinators, resulting in massive population declination [4,5]. Thus, it is urgent to develop efficient strategies to prevent the pollinators from insecticides including three leading categories of organophosphates, pyrethroids, and neonicotinoids [6–8].

Currently, most approaches for pollinator protection focus on removing the insecticides from the contaminated drinking water and crop. Ni et al. reported that a surface discharge cold plasma oxidation technology could generate reactive oxygen species and thus degrade imidacloprid insecticide in the drinking water for bees, resulting in significant decrease of mortality to 35% after 7 days of exposure[9]. Halik et al. presented a facile approach to remove organophosphorus compounds from water using magnetic Fe_3O_4 nanoparticles, in which the molecular binding between phosphonic acid of organophosphorus and metal oxides induced fast compound scavenging from artificial and real water samples, while the magnetic property of magnetic nanoparticles enabled a facile collection[10]. Taking advantage of specific binding of acetylcholinesterase (AChE) on erythrocyte membranes with organophosphate, cell membrane-coated nanosponges and nanoparticles were developed and exhibited effective removal and neutralization of organophosphorus insecticides[11,12]. The above reported methods while affording certain benefits to decrease survival stress of pollinators are not appropriate for scavenging the insecticides in the bodies of pollinators. Recently, Chen et al. developed calcium carbonate microspheres encapsulated with phosphotriesterase as a detoxification formulation to scavenge organophosphate insecticides in managed bees via enzymatic degradation of malathion, affording a direct technique to mitigate organophosphate damage to pollinator colonies[13]. Considering that multiclass insecticides have been extensively employed to increase crop production and quality in modern agriculture, scavengers with potent removal capacity, facile construction, and towards broad-spectrum insecticides is a better alternative to tackle the exposure of pollinators to a cocktail of insecticides in agriculture processes.

Herein, we have developed versatile and potent insecticide scavengers based on locust cell membrane and tannic acid (TA)-coated mesoporous silicon microparticles (MTSM) to protect managed pollinators from varying insecticides (Fig. 1). Besides high surface area, accessible modification, and superb safety, mesoporous silicon microparticles (SM) afford immense space for cargo packing[14–16]. TA as a natural polyphenol provides multiple pyrogallol for robust surface modification and drug encapsulation via covalent conjugation and π-π stacking[17–22]. Locust cell membrane was reported to have strong affinity with insecticides through selective degradation of organophosphorus (OP) by acetylcholinesterase (AChE)[11,23,24], and specific binding of neonicotinoid (NNI) and pyrethroid (PY) with nicotine receptors of acetylcholine (nAChRs) and voltage-gated sodium channels(VGSCs), respectively[25–28]. MTSM was designed to accomplish the removal of broad-spectrum insecticides and minimize nonspecific interactions with favorable enzymes exsisting in gastrointestinal system of bees. Of note, MTSM

exhibited over 12 h residency in gastrointestinal tract of bumblebees to facilitate insectide scanvenging, and induced dose-dependent detoxicification effect in bumblebee fed with insecticide-contaminated pollen patties, affording a remarkably elevated survival rate up to 90%. This potent, versatile and broad-spectrum detoxification strategy holds tremdous potential to tackle the exposure of pollinators to diverse insecticides dominantly used in agriculture processes.

Results and Discussion

Fabrication of MTSM

Tannic acid-coated microparticles (TSM) was fabricated through the covalent conjugation of TA with amino groups of mesoporous silicon microparticles via Schiff base and Michael addition chemistry. The characteristic signals of hydroxyl group at 3500 cm^{-1}, carbonyl group at 1720 cm^{-1}, and phenyl group at 1530–1620 cm^{-1} in FT-IR spectra (Fig. 2a) signified the successful introduction of TA on SM. Moreover, TSM with varying amount of TA (0.76-12.0 wt%) could be readily acquired by adjusting the feed ratios of TA to SM as characterized by thermogravimetric (Fig. 2b, Supplementary Fig. 1) and bicinchoninic acid (BCA, Fig. 2c) assays, in which the TA amount increased with elevating the TA/SM weight ratios, and reached a plateau when the TA/SM weight ratio was higher than 0.2. The locust cell membrane featured with various binding sites of different insecticides has been utilized to selectively recognize the insecticides released from polluted pollen[29,30]. The coating of locust cell membrane on TSM was facilely accomplished under mild ultrasound condition to form MTSM. Confocal imaging revealed that obvious red rings derived from fluorescent probe DiD inserted in locust cell membrane clearly appeared on the microparticles (Fig. 2d-e), signifying the successful membrane coating. The membrane amount on MTSM could be adjusted by changing the concentrations of cell membrane that quantified with membrane proteins, and nearly attained the maximum when the protein concentration increased to 0.25 mg/mL (Fig. 2f). The bioactivity of AChE on microparticles was determined through monitoring the degradation of acetylthiocholine into thiocholine by AChE as previous reports (Fig. 2g) [31–33], and the results revealed that the process of membrane coating induced negligible change of the catalytic activity of AChE in cell membrane towards acetylthiocholine (Fig. 2h). N_2 adsorption isotherms revealed that both MTSM and TSM possessed slightly decreased pore volume with average pore sizes ranging from 5–20 nm (Fig. 2i, Supplementary Fig. 2), providing accessible space for drug adsorption. Porous surface morphology of microparticles following the TA and cell membrane coating was further revealed by scanning electron microscopy (SEM) images (Fig. 2J).

In vitro removal efficiency of insecticides by MTSM

Over one third of insecticides in use are OP insecticides which cause high accumulation and toxicity towards pollinators[34,35]. Here, triazophos (TZP), methyl parathion (MPT), and chlorpyrifos (CP) were employed as typical examples of OP (Supplementary Fig. 3) to evaluate the removal efficiency. Leveraging the strong π-π stacking between OP insecticides and TA as well as biomimetic recognition

and binding of OP insecticides by AChE, MTSM was expected to afford efficient insecticide scavenging (Fig. 3a). π-π stacking has been utilized to accomplish robust drug loading in varying drug delivery systems including micelles, polymersomes, nanoparticles[36–39]. Figure 3b exhibited that increasing the TA/SM ratios benefited the removal of TZP, in which the removal efficiency reached a plateau when the TA/SM weight ratios was higher than 0.2. The decoration of locust cell membrane on microparticles further improved the drug absorption, and a membrane protein concentration of no lower than 0.25 mg/mL afforded a removal efficiency of over 83% (Fig. 3c). Thus, MTSM constructed at a TA/SM weight ratio of 0.2 and a membrane protein concentration of 0.25 mg/mL was utilized for the evaluation of the effect of removal time, microparticle and insecticide concentrations. As expected, the TZP adsorption was enhanced with increasing MTSM concentrations, while modest increase (around 4%) of removal efficiency was obtained when the MTSM concentrations increased from 20 to 40 mg/mL (Fig. 3d). Figure 3e demonstrated that MTSM afforded efficient removal of TZP at a wide range of TZP concentrations from 0.01 to 0.5 mg/mL. More importantly, MTSM provided swift TZP removal with over 57% drug clearance within 5 min, and the removal efficiency could reach around 95% after 12 h incubation (Fig. 3f). MSM formed by coating SM with cell membrane only was used to explore the cell membrane effect on drug clearance. Regardless of incubation time, microparticle and drug concentrations, the removal efficiency was in the order: MTSM > TSM > > MSM > SM. Removal mechanism of MTSM related to TA and cell membrane was further explored. Of note, remarkable red shift from 278 to 290 nm of TZP induced by TA in UV-vis spectra (Fig. 3g) indicated that strong π-π stacking occurred between TZP and TA. Spontaneous interaction between TA and TZP revealed by the low negative Gibbs energy (ΔG=-20 kJ/mol) was further confirmed by isothermal titration calorimetry (ITC, Fig. 3h-i). The binding process was also accompanied with heat absorption (ΔH = 2184 kJ/mol) and entropy increment (ΔS = 7396 J/mol·K) that may be attributed to the intermolecular reaction including π-π stacking. AChE was reported to be responsible for recognition and degradation of OP insecticides[11,12], and the degradation reaction of TZP triggered by AChE was illustrated in Fig. 3j. Following the incubation of TZP with MTSM, the significantly reduced TZP, and the appearance and increased phenyltriazolol with time was measured by HPLC (Fig. 3k), corroborating that TZP was efficiently degraded by AChE on the microparticles. Apart from the direct physical absorption mediated by TA, enzymatic degradability of AChE towards TZP greatly benefits the insecticide detoxification. Furthermore, MPT and CP as two conventional OP insecticides were utilized to further evaluate the removal capacity of microparticles towards OP insecticides, and the results demonstrated that both MTSM and TSM could efficiently scavenge the insecticides (Fig. 3l). In comparison with TSM and MSM, MTSM generated much higher removal efficiency of around 80% towards MPT and CP.

Compared with conventional OP insecticides, NNI and PY insecticides as advanced insecticides exhibited even more toxicity towards bees and other crop pollinators characterized by much lower LD_{50}[7]. Imidacloprid (IMI) was employed as a typical example of NNI insecticides to evaluate the scavenging capacity, and the results showed that the removal efficiency of microparticles was markedly elevated with the introduction of TA and reached a plateau of 43.1% when the TA/SM weight ratios were higher than 0.2 (Fig. 4a). Neonicotinoids and pyrethroids were reported to bind the nAChRs and VGSCs on the

insect cell membrane, respectively to kill insects[40]. MTSM presented nearly 10.0 μg/g of nAChRs and 5.2 μg/g of VGSCs on the surface when the concentration of locust cell membrane proteins was 0.25 mg/mL (Fig. 4b), indicating that microparticles decorated with cell membrane might improve the drug absorption. Indeed, over 55% removal efficiency for IMI was attained when the membrane protein on MTSM was 0.25 mg/mL (Fig. 4c). Thereafter, MTSM constructed as above was utilized for the evaluation of the effect of removal time, pH, microparticle and insecticide concentrations. As expected, the IMI adsorption was enhanced with increasing microparticle concentrations and reached 67.1% when the MTSM concentration was 40 mg/mL (Fig. 4d). Furthermore, MTSM could maintain high removal efficiency even at a high IMI concentration of 0.5 mg/mL (Fig. 4e), and the removal efficiency increased with treatment time and reached 77.3% at 48 h (Fig. 4f). Of note, decreasing pH to 4.8 showed little influence on the absorption efficiency (Fig. 4g), suggesting that the removal efficiency of insecticides by MTSM would not be compromised in the stomach and gut of bees (pH 4.8–6.5). Similarly, MTSM and TSM exhibited efficient scavenging of other NNI insecticides (acetamiprid, thiamethoxam), in which MTSM revealed a removal efficiency of around 45.2% for acetamiprid (Fig. 4h). Meanwhile, we assessed the scavenging capacity of PY by microparticles using chlorpyrifos as a typical example, and the result displayed that around 50% of chlorpyrifos was removed by MTSM within 60 min (Fig. 4i, Supplementary Fig. 4), corroborating their broad-spectrum scavenging capacity towards varying insecticide.

Inhibition of nonspecific adsorption

The ideal insecticide scavengers should not only possess potent removal capacity, but also minimize the adsorption of favorable substances in gastrointestinal system of pollinators (Fig. 5a). Sucrase, protease, and amylase are crucial digestive enzymes and generally present in gastrointestinal system of bees[41]. As shown in Fig. 5b-d, obvious adsorption of sucrase, protease, and amylase was observed in TSM owing to the interactions of enzymes with TA on the surface of microparticles. In sharp contrast, MTSM displayed significantly decreased absorption of all enzymes at concentrations varying from 1.0 to 100 μg/mL, signifying the introduction of cell membranes extraordinarily inhibited the nonspecific clearance of favorable enzymes. A mixture of TZP and enzymes was prepared to mimic the GI environment of bees for the exploration of insecticide removal using microparticles. In comparison with TSM, MTSM presented obviously enhanced TZP removal while significantly decreased adsorption of sucrase (15% VS 27%), amylase (17% VS 48%), and protease (14% VS 42%) (Fig. 5e). The potent insecticide clearance and minimum adsorption of favorable enzymes (< 20%) support the outstanding efficiency and safety of MTSM.

In vivo gastrointestinal distribution

MTSM was labeled with FITC (FITC-MTSM) through the reaction of FITC with amino group of SM to track the distribution and metabolism in GI of pollinators. After feeding bumblebees with FITC-MTSM for 30 minutes, MTSM was observed to sequentially pass through the crop stomach, proventriculus, midgut and hindgut of the GI tract with time. During the initial period of digestion, most microparticles were distributed in the crop stomach, and negligible dissemination of microparticles was observed in the

midgut and hindgut. Then, the majority of FITC-MTSM moved out of the crop stomach and reached midgut after 4 h (Fig. 6a). Notably, a significant number of microparticles existed in the midgut and hindgut of the GI tract from 4 to 12 h (Fig. 6b-c). Pollen grains were reported to be similarly digested in the ventriculus for around 12 h[42,43], thus facilitating the absorption of insecticides in pollen by MTSM in the GI tract of bees. After 48 h, no fluorescent microparticles was observed in crop stomach, proventriculus, midgut and hindgut of the GI tract, supporting that all microparticles were excreted from bees within 48 h (Fig. 6d).

In vivo detoxification efficacy

Bumblebees (n = 20) fed with MTSM at varying concentrations of 0.1–50 mg/mL in sucrose solution (2.0 g/mL) all survived within 10 days (Supplementary Fig. 5), signifying the remarkable safety of MTSM. The in vivo detoxification efficacy was evaluated in bumblebees fed with insecticide-contaminated pollen balls. Initially, pollen balls containing different concentrations of TZP (3, 15, 60, 120 μg/g) were employed to determine the levels of insecticide toxicity, and the results revealed that pollen balls containing 60 and 120 μg TZP/g caused 100% mortality at day 4 and 1 (Supplementary Fig. 6), and thus were employed for the assessment of moderate and acute toxicity, respectively. At the moderate level of toxicity (60 μg TZP/g in pollen), TSM and MTSM treatment largely decreased the incidence of mortality and presented 60% and 70% survival rate within 10 days at a low concentration of 1.0 mg/mL in sucrose, respectively (Fig. 7b). As expected, increasing the concentration of microparticles to 20 mg/mL generated better detoxification effect with a survival rate up to 90%. At the acute toxicity condition (120 μg TZP/g in pollen), both TSM and MTSM induced extended survival time, in which bumblebees in TSM group all died after 7 days while those in MTSM group presented 15% survival rate even 10 days later (Fig. 7c, Supplementary Fig. 7). The survival rate could be further increased to 60% when a higher microparticle concentration of 20 mg/mL was employed.

OP was reported to induce ACh massive accumulation and neurotoxicity by inhibiting carboxyl ester hydrolases like AChE in different insects including pollinators[44,45]. To explore the protection capacity of MTSM towards AChE bioactivity in bees, homogenized bumblebee cell fragments were incubated with the supernatants of mixed TZP and microparticles (Fig. 7d). With increasing concentrations of microparticles, higher retention of AChE activity was obtained (Fig. 7e). For MTSM, the retention activity of AChE reached over 80% when the microparticle concentration was higher than 5 mg/mL, and nearly complete activity retention (around 99%) was acquired at a MTSM concentration of 40 mg/mL, indicating a dose-dependent protection of AChE by MTSM.

Besides OP, NNI insecticides like imidacloprid (IMI) was employed to explore the in vivo detoxification capacity of microparticles. It should be noted that IMI presented much higher toxicity than TPZ, and pollen balls containing 15 μg IMI/g (acute toxicity) and 5 μg IMI/g (moderate toxicity) induced complete death of bumblebees within 1 and 3 days, respectively (Fig. 7f-g). MTSM demonstrated apparent detoxification efficacy towards moderate and acute toxicity in bumblebees. For bumblebees fed with pollen balls containing 5 μg IMI/g, MTSM at a concentration of 20 mg/mL in sucrose afforded a high

survival rate of 95%. Thus, MTSM afforded potent in vivo scavenging capacity of broad-spectrum insecticides in pollinators.

Conclusions

We have demonstrated that versatile and potent insecticide scavengers constructed through facile surface decoration of mesoporous silicon microparticles with tannic acid (TA) and locust cell membrane sequentially (MTSM) afford effective protection of pollinators from a broad-spectrum insecticides including organophosphorus, pyrethroids, and neonicotinoids. Leveraging the π-π stacking with TA and specific binding by the acetylcholinesterases, nicotine receptors of acetylcholine, or voltage-gated sodium channels on locust cell membrane, MTSM induced markedly improved removal of various insecticides while minimum nonspecific clearance of favorable enzymes mainly exsisting in gastrointestinal system of pollinators. MTSM could be almost entirly excreted from bees within 48 h, and caused no death of bees even at a high concentration of 50 mg/mL, signifying the excellent safety. With over 12 h residency in gastrointestinal tract of bumblebees, MTSM exhibited extensive insectide scavenging, affording dose-dependent detoxicification efficacy towards multiple insecticides and significantly elevated survival rate up to 90%. Although more research such as field-wide bee colony survival test and pollination efficiency of crops after treatment should be further conducted, MTSM featured with versatility and potency in detoxification of pollinators has shown a great potential in translation, which might benefit sustainable agriculture worldwide.

Experimental Section

Materials

Mesoporous silica microparticles with amino groups on the surface (SM, Suzhou NanoMicro Technology Co., Ltd, China), tannic acid (TA, > 98%, Sigma-Aldrich, Germany), triazophos (TZP, > 99%, Shanghai Titan Scientific Co., Ltd, China), methyl parathion (MPT, > 99%, Shanghai Titan Scientific Co., Ltd, China), chlorpyrifos (CP, > 99%, Shanghai Macklin Biochemical Co., Ltd, China), imidacloprid (IMI, > 99%, Shanghai Macklin Biochemical Co., Ltd, China), thiamethoxam (TMX, > 99%, Shanghai Macklin Biochemical Co., Ltd, China), acetamiprid (ACM, > 99%, Shanghai Macklin Biochemical Co., Ltd, China), cyfluthrin (CFT, > 99%, Shanghai Titan Scientific Co., Ltd, China), phenyl methane sulfonyl fluoride (PMSF, Beyotime Biotech Inc, China), cell membrane red fluorescent probe (DiD, Beyotime Biotech Inc, China), fluorescein isothiocyanate (FITC, Shanghai Macklin Biochemical Co., Ltd, China) and 5,5'-dithiobis-2-nitrobenzoic acid (DTNB, Shanghai Aladdin Biochemical Technology Co., Ltd, China) were used as received. 4-hydroxyethyl piperazine ethanesulfonic acid (HEPES, > 99.5%, Sigma-Aldrich, Germany), tris(hydroxymethy)amino- methane hydrochloride (Tris-HCl, > 99%, Sigma-Aldrich, Germany) and phosphate buffered saline (PBS, > 99%, Sigma-Aldrich, Germany) were the buffer systems. Pierce™ BCA protein assay kit (Beyotime), membrane and cytosol protein extraction kit (Beyotime), insect amylase ELISA kit (Meimian), insect protease ELISA kit (Meimian), and insect sucrase ELISA kit (Meimian) were

used according to the instructions. All other reagents and solvents purchased from Sinopharm Chemical Reagent Co., Ltd. and used as received.

Characterization

Fourier transform infrared (FTIR) spectra were recorded in the wavenumber range of 500–4000 cm^{-1} using FTIR spectroscopy (Tensor 27, Bruker, Germany). The surface morphology of the microparticles was observed using scanning electron microscope (SEM, Hitachi SU8010, Japan). Surface area and pore size analyzer (ASAP2460, Micromeritics, America) was used to analyze the pore size and pore volume of microparticles. The degassing temperature was 120 ℃ and the degassing time was 12 h. The concentrations of insecticides were detected by high performance liquid chromatograph (HPLC, ProStar LC240, Waters Alliance HPLC) equipped with a C18 analytical column. The column temperature was set at 30 ℃, the flow rate was 1.0 mL/min, the injection volume was 10 μL, the mobile phase was acetonitrile/ water (65/35, v/v), and the UV detection wavelength was 230 nm (TZP, MPT), 245 nm (CP), and 270 nm (IMI, CFT). Multifunctional microplate reader (Varioskan LUS, Thermo Fisher Scientific, America) was used for the measurement of AChE activity.

MTSM Preparation

MTSM was prepared through sequential surface decoration of mesoporous silicon microparticles (SM) with tannic acid (TA) and locust cell membrane. Firstly, TA-decorated SM (TSM) was obtained by the covalent conjugation of TA with amino group of SM. Briefly, a TA solution in HEPES was added into 100 mg of SM dispersed in HEPES buffer (20 mL, 5 mM, pH = 7.4). The TA/SM weight ratios were fixed at 0.01, 0.1, 0.2, 0.5, and 1. After stirring at room temperature for 12 h, the reaction solution was centrifuged at 6000 rpm for 6 min and washed with phosphate buffered saline (PBS, 10 mM, pH 7.4) for three times. Then, the obtained dispersion was reacted with two-fold excessive $NaBH_4$ at room temperature for 4 h. After sequential centrifuging, washing with PBS, and drying at 35°C in a vacuum oven, TSM product was obtained. Yield: 95.6%. FTIR: 3350 cm^{-1} (-OH, v), 1720 cm^{-1} (C = O, v), 1530 and 1619 cm^{-1} (C-C, C = C of benzyl group, v).

Differential centrifugation method was utilized to extract the locust cell membrane[46–48]. Briefly, the living locusts were frozen under liquid nitrogen, sterilized in 75% ethanol, grinded, and filtered with a cell strainer (70 μm) to obtain cell suspension. To 20 million of extracted locust cells, 1.0 ml of membrane protein extraction solution was added according to membrane and cytosol protein extraction kit. Phenylmethylsulfonyl fluoride (PMSF) as a protease inhibitor was introduced within a few minutes at a final concentration of 1.0 mM to maintain the activity of the proteins on cell membrane. After shaking for 30 min in an ice-water bath, the mixture was repeatedly frozen and thawed thrice to disrupt the cells. Then, the membrane fragments were separated using differential centrifugation and stored at -80 ℃ until use. The total protein content in membrane fragments was quantified by a Pierce™ BCA protein

assay kit. The locust cell membrane was coated on TSM by using ultrasound machine (FB15063, Fisherbrand, America) with a power of 100 W in ice-water bath for 15 min. The concentrations of membrane proteins varied from 0 to 1.0 mg/mL. To observe the membrane coating, DiD stained MTSM (DiD-MTSM) was prepared by adding 0.5 wt% of DiD (excitation/emission = 644/665 nm) into locust cell membrane solution, and then was coated on microparticles by gentle sonication.

Measurement of AChE activity.

AChE activity assay was performed in accordance with a previously described protocol[31,32]. In short, a working solution of 100 mM Tris-HCl, 20 mM KCl, 2.0 mM DTNB, and 2.0 mM acetylthiocholine was prepared. Then, 100 μL of working solution was mixed with equivalent volume of cell membrane solution containing AChE in a 96-well plate. UV absorbance of the reduced phenyltriazolol product at 412 nm was recorded using a Varioskan Lux multimode reader every 1 min for 20 min to determine the change of AChE activity.

Insecticide Removal

Different OP insecticides including triazophos (TZP), methyl parathion (MPT), and chlorpyrifos (CP) was employed to evaluate the scavenging capacity of MTSM. Firstly, simulated intestinal fluid (SIF, pH 6.5) was prepared by dissolving KH_2PO_4 (6.8 g, 50 mM) and NaOH (0.9 g, 22.5 mM) in distilled H_2O (1.0 L). Then, MTSM was mixed with OP insecticides in SIF via gentle vortex at 37 ℃. After centrifuging at 6000 rpm for 6 min, the remained insecticides in supernatant was quantified by high performance liquid chromatography (ProStar LC240, Waters Alliance HPLC). The removal efficiency of OP insecticides was calculated with the formula: removal efficiency (%) = (1-OP insecticides in supernatant/feed OP insecticides) × 100%. The effect of OP insecticides concentration (0.01–0.5 mg/mL), microsphere concentration (2.0–40 mg/mL), and mixing time (5.0-720 min) on removal efficiency was investigated in detail. All experiments were performed in triplicate. The removal capacity of MTSM towards neonicotinoids and pyrethroids was similarly investigated except that HPLC with a detect wavelength at 270 nm was utilized for quantification.

Mechanism of OP insecticides removal

The π-π interactions between OP insecticides and microspheres were investigated by monitoring the bathochromic shift of absorption peak generated by mixing TZP (20 μg/mL) and TA (20 μg/mL) solution. The interaction forces between TA and TZP molecules was determined by isothermal titration calorimetry (ITC, TA, America). The binding and neutralization of OP insecticides with AChE on microspheres was monitored by measuring the leaving group phenyltriazolol. After mixing the microparticles (20 mg/mL) with TZP (50 μg/mL) for 5, 15, 60, or 120 min, the supernatant was collected and the amount of TZP and phenyltriazolol was quantified with HPLC.

In vitro detoxification effect

In vitro detoxification effect was assessed by measuring the activity retention of AChE on bumblebee cell membrane, following the treatment with the supernatant of the mixture of TZP and MTSM solution. Typically, TZP (50 μg/mL) was mixed with MTSM (2, 5, 10, 20, 40 mg/mL) at room temperature for 1 h. After centrifuging at 12000 g for 30 min, 200 μL of supernatant was mixed with equivalent volume of the bumblebee cell membrane solution. The AChE activity was determined as described above.

Inhibition of nonspecific adsorption

Sucrase, protease, and amylase existing in gastrointestinal tract of bumblebees were utilized to evaluate the inhibition of nonspecific adsorption by MTSM. The MTSM solution (20 mg/mL) was mixed with different enzymes (1 ~ 100 μg/mL) for 1 h at 37℃. After centrifuging at 6000 rpm for 6 min, the activity of enzymes in supernatant was determined by corresponding enzyme kit.

In vivo biodistribution

FITC labeled MTSM (FITC-MTSM) was prepared by the reaction of FITC with amino group on the surface of microparticles, followed by the coating with locust cell membrane. After starving for 3 h, twenty of bumblebees were fed with 1.0 mg/mL FITC-MTSM in sucrose (2.0 g/mL) for 30 min. Then, the bumblebees were beheaded using dissection scissors at 0, 4, 12, 48 h. GI tracts were collected and placed on a glass slide for fluorescence imaging (490 nm) using a microscope (Eclipse, Nikon, Japan).

In vivo detoxification efficacy

Pollen balls were prepared by mixing various insecticides with 10 g of high-desert bee pollen granules, followed by shaking until a homogeneous slurry was formed and full absorption of insecticides. The insecticide-containing pollens was rolled with sucrose into pollen ball by hand to obtain contaminated pollen balls. Microparticles dispersed in a sucrose solution (2 g/mL) were prepared as scavenging agents. Bumblebees (20/group) placed in microcolony-rearing cages were treated with the contaminated pollen balls and the microparticles-based scavenging agents simultaneously. Microcolonies were observed every 12 h for mortality monitor until all bees deceased or 10 d elapsed.

Declarations

Acknowledgments

This work was supported by grants from the National Key R&D Program of China (No. 2022YFB3804600), the National Natural Science Foundation of China (No. 82305052, 52373299), Young

Elite Scientists Sponsorship Program by CAST (2022-QNRC1-04) and the Jiangsu Specially-Appointed Professors Program (No. 013074004038).

References

1. Lemanski, N. J., Williams, N. M. & Winfree, R. Greater bee diversity is needed to maintain crop pollination over time. *Nat. Ecol. Evol.* **6**, 1516-1523 (2022).
2. Bascompte, J. & Scheffer, M. The Resilience of Plant–Pollinator Networks. *Annu. Rev. Entomol.* **68**, 363-380 (2023).
3. Garibaldi, L. A., Requier, F., Rollin, O. & Andersson, G. K. S. Towards an integrated species and habitat management of crop pollination. *Curr. Opin. Insect Sci.* **21**, 105-114 (2017).
4. Goulson, D., Nicholls, E., Botías, C. & Rotheray, E. L. Bee declines driven by combined stress from parasites, pesticides, and lack of flowers. *Science* **347**, 10 (2015).
5. Varah, A. et al. The costs of human-induced evolution in an agricultural system. *Nat. Sustain.* **3**, 63-71 (2020).
6. Fu, H. Y. et al. Advances in organophosphorus pesticides pollution: Current status and challenges in ecotoxicological, sustainable agriculture, and degradation strategies. *J. Hazard. Mater.* **424**, 20 (2022).
7. Osaka, A. et al. Exposure characterization of three major insecticide lines in urine of young children in Japan-neonicotinoids, organophosphates, and pyrethroids. *Environ. Res.* **147**, 89-96 (2016).
8. Zhang, X. D. et al. Environmental occurrence, toxicity concerns, and biodegradation of neonicotinoid insecticides. *Environ. Res.* **218**, 15 (2023).
9. Ni, J. B. et al. Efficient degradation of imidacloprid by surface discharge cold plasma: Mechanism of interaction between ROS and molecular structure and evaluation of residual toxicity. *J. Hazard. Mater.* **465**, 12 (2024).
10. Park, H. et al. Magnetite nanoparticles as efficient materials for removal of glyphosate from water. *Nat. Sustain.* **3**, 129-135 (2020).
11. Chen, Y. J. et al. Cell-membrane-cloaked oil nanosponges enable dual-modal detoxification. *ACS Nano* **13**, 7209-7215 (2019).
12. Zou, S. J. et al. Dual-modal nanoscavenger for detoxification of organophosphorus compounds. *ACS Appl. Mater. Interfaces* **14**, 42454-42467 (2022).
13. Chen, J. et al. Pollen-inspired enzymatic microparticles to reduce organophosphate toxicity in managed pollinators. *Nat. Food* **2**, 339-347 (2021).
14. Vallet-Regí, M., Schüth, F., Lozano, D., Colilla, M. & Manzano, M. Engineering mesoporous silica nanoparticles for drug delivery: where are we after two decades? *Chem. Soc. Rev.* **51**, 5365-5451 (2022).
15. Feng, Y. et al. Mesoporous silica nanoparticles-based nanoplatforms: basic construction, current state, and emerging applications in anticancer therapeutics. *Adv. Healthc. Mater.* **12**, 16 (2023).

16. Li, X. D. et al. ROS-responsive Janus Au/mesoporous silica core/shell nanoparticles for drug delivery and long-term CT imaging tracking of MSCs in pulmonary fibrosis treatment. *ACS Nano* **17**, 6387-6399 (2023).
17. Cui, C. Y. & Liu, W. G. Recent advances in wet adhesives: Adhesion mechanism, design principle and applications. *Prog. Polym. Sci.* **116**, 34 (2021).
18. Yang, Y. et al. Ultra-durable cell-free bioactive hydrogel with fast shape memory and on-demand drug release for cartilage regeneration. *Nat. Commun.* **14**, 7771 (2023).
19. Li, Z. et al. A multifunctional nanoparticle mitigating cytokine storm by scavenging multiple inflammatory mediators of sepsis. *ACS Nano* **17**, 8551-8563 (2023).
20. Zhang, Y. et al. Functional and binding studies of gallic acid showing platelet aggregation inhibitory effect as a thrombin inhibitor. *Chin Herb Med* **14**, 303-309 (2022).
21. Ta, W. et al. Comparison of intestinal absorption characteristics between rhubarb traditional Chinese medicine preparation and activity ingredients using in situ and in vitro model. *Chin Herb Med* **15**, 117-122 (2023).
22. Fu, M. et al. Cancer treatment: from traditional Chinese herbal medicine to the liposome delivery system. *Acta Materia Medica* **1**, 486-506 (2022).
23. Čadež, T., Kolić, D., Šinko, G. & Kovarik, Z. Assessment of four organophosphorus pesticides as inhibitors of human acetylcholinesterase and butyrylcholinesterase. *Scientific Reports* **11**, 21486 (2021).
24. Yang, L. M., Qu, L. J., Zhang, X. L., Li, M. M. & Liu, Z. Aptamer-induced in-situ growth of acetylcholinesterase-$Cu_3(PO_4)_2$ hybrid nanoflowers for electrochemical detection of organophosphorus inhibitors. *Nano Res.* **16**, 12134-12143 (2023).
25. Perry, T. et al. Role of nicotinic acetylcholine receptor subunits in the mode of action of neonicotinoid, sulfoximine and spinosyn insecticides in Drosophila melanogaster. *Insect Biochemistry and Molecular Biology* **131**, 103547 (2021).
26. Thany, S. H. Molecular mechanism of action of neonicotinoid insecticides. *Int. J. Mol. Sci.* **24**, 4 (2023).
27. O'Reilly, A. D. & Stanley, D. A. Solitary bee behaviour and pollination service delivery is differentially impacted by neonicotinoid and pyrethroid insecticides. *Sci. Total Environ.* **894**, 9 (2023).
28. Soderlund, D. M. in *Advances in Neurotoxicology* Vol. 4 (eds Michael Aschner & Lucio G. Costa) 113-165 (Academic Press, 2020).
29. Zhang, J. et al. RNA interference revealed the roles of two carboxylesterase genes in insecticide detoxification in Locusta migratoria. *Chemosphere* **93**, 1207-1215 (2013).
30. Huang, Z. et al. Insect transient receptor potential vanilloid channels as potential targets of insecticides. *Developmental & Comparative Immunology* **148**, 104899 (2023).
31. Ellman, G. L., Courtney, K. D., Andres, V. & Featherstone, R. M. A new and rapid colorimetric determination of acetylcholinesterase activity. *Biochem. Pharmacol.* **7**, 88-90 (1961).

32. Vlogiannitis, S. et al. Reduced proinsecticide activation by cytochrome P450 confers coumaphos resistance in the major bee parasite Varroa destructor. *Proc. Natl. Acad. Sci. U. S. A.* **118**, 7 (2021).
33. Chen, Q. et al. MOF-derived Co_3O_4@Co-Fe oxide double-shelled nanocages as multi-functional specific peroxidase-like nanozyme catalysts for chemo/biosensing and dye degradation. *Chem. Eng. J.* **395**, 125130 (2020).
34. Cappa, F., Baracchi, D. & Cervo, R. Biopesticides and insect pollinators: Detrimental effects, outdated guidelines, and future directions. *Sci. Total Environ.* **837**, 155714 (2022).
35. Ma, X. J. et al. Multifunctional Fe-doped carbon dots and metal-organic frameworks nanoreactor for cascade degradation and detection of organophosphorus pesticides. *Chem. Eng. J.* **464**, 10 (2023).
36. Shi, Y. et al. Π-Π Stacking Increases the Stability and Loading Capacity of Thermosensitive Polymeric Micelles for Chemotherapeutic Drugs. *Biomacromolecules* **14**, 1826-1837 (2013).
37. Gu, X. et al. cRGD-decorated biodegradable polytyrosine nanoparticles for robust encapsulation and targeted delivery of doxorubicin to colorectal cancer in vivo. *J. Control. Release* **301**, 110-118 (2019).
38. Xie, J. G. et al. Codelivery of BCL2 and MCL1 inhibitors enabled by phenylboronic acid-functionalized polypeptide nanovehicles for synergetic and potent therapy of acute myeloid leukemia. *Adv. Sci.* **10**, 14 (2023).
39. Song, Y. et al. An integrated quorum quenching biocatalytic nanoplatform for synergistic chemo-photothermal eradication of P. aeruginosa biofilm infections. *Acta Biomaterialia* **171**, 532-542 (2023).
40. Yang, Y. Y. et al. Global honeybee health decline factors and potential conservation techniques. *Food Secur.* **15**, 855-875 (2023).
41. Ma, W. H. Comparative study on the activity of digestive enzymes in salivary gland and midgut of Italian honeybee workers. *Agriculture Handbook* **30**, 724-727 (2011).
42. Aylanc, V., Falcão, S. I. & Vilas-Boas, M. Bee pollen and bee bread nutritional potential: Chemical composition and macronutrient digestibility under in vitro gastrointestinal system. *Food Chemistry* **413**, 135597 (2023).
43. Brys, M. S., Skowronek, P. & Strachecka, A. Pollen diet-properties and impact on a bee colony. *Insects* **12**, 9 (2021).
44. Ganie, S. Y., Javaid, D., Hajam, Y. A. & Reshi, M. S. Mechanisms and treatment strategies of organophosphate pesticide induced neurotoxicity in humans: A critical appraisal. *Toxicology* **472**, 153181 (2022).
45. Pulkrabkova, L. et al. Neurotoxicity evoked by organophosphates and available countermeasures. *Arch. Toxicol.* **97**, 39-72 (2023).
46. Zhang, Q. Z. et al. Neutrophil membrane-coated nanoparticles inhibit synovial inflammation and alleviate joint damage in inflammatory arthritis. *Nat. Nanotechnol.* **13**, 1182-1190 (2018).

47. Liu, L. Z. et al. Systematic design of cell membrane coating to improve tumor targeting of nanoparticles. *Nat. Commun.* **13**, 15 (2022).
48. Ma, J. N. et al. Tumor microenvironment targeting system for glioma treatment via fusion cell membrane coating nanotechnology. *Biomaterials* **295**, 10 (2023).

Figures

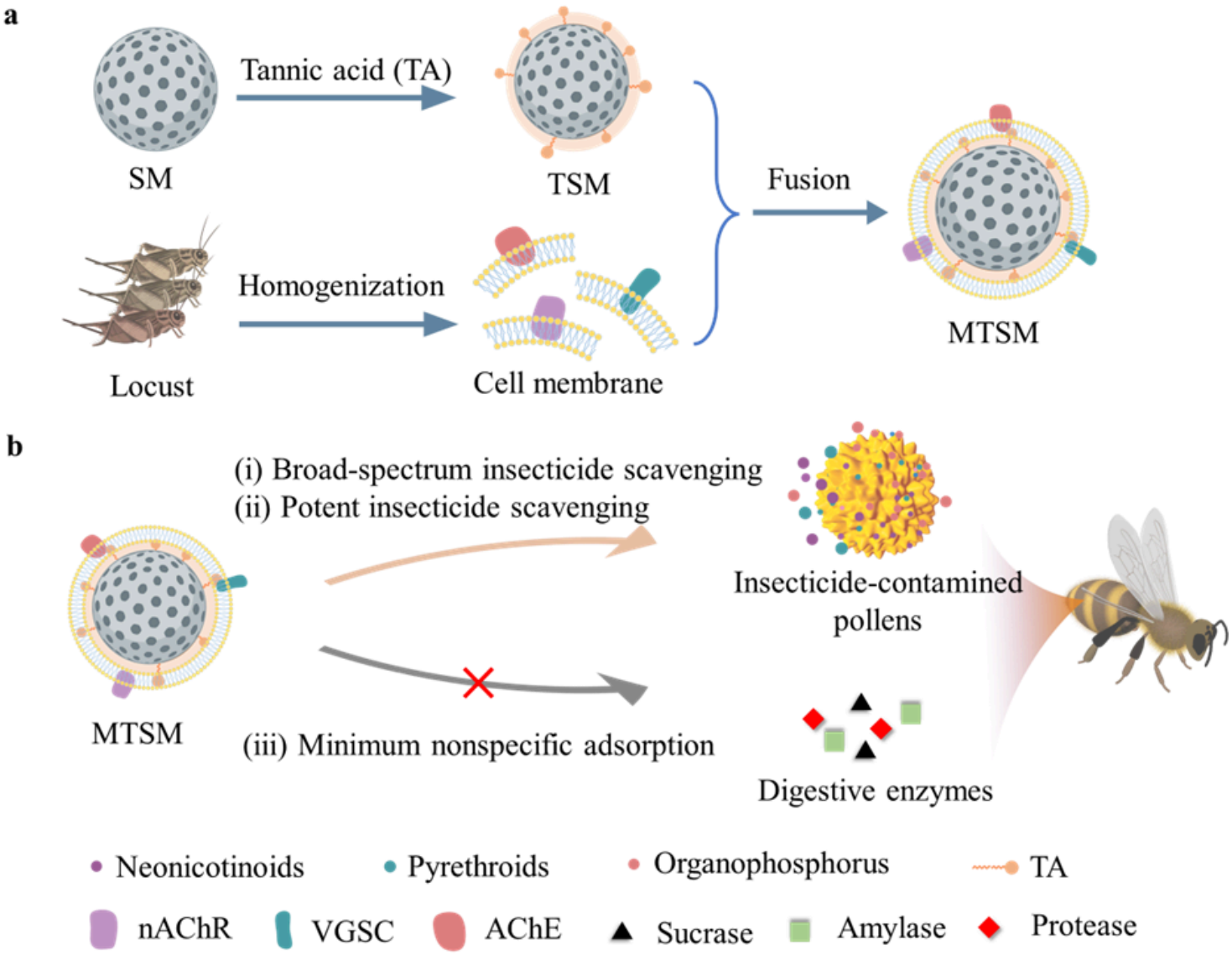

Figure 1

Schematic illustration of construction and insecticide scavenging of tannic acid and locust cell membrane-adapted mesoporous silicon microparticles (MTSM). a, MTSM construction. **b,** Selective insecticide scavenging from pollinators by MTSM.

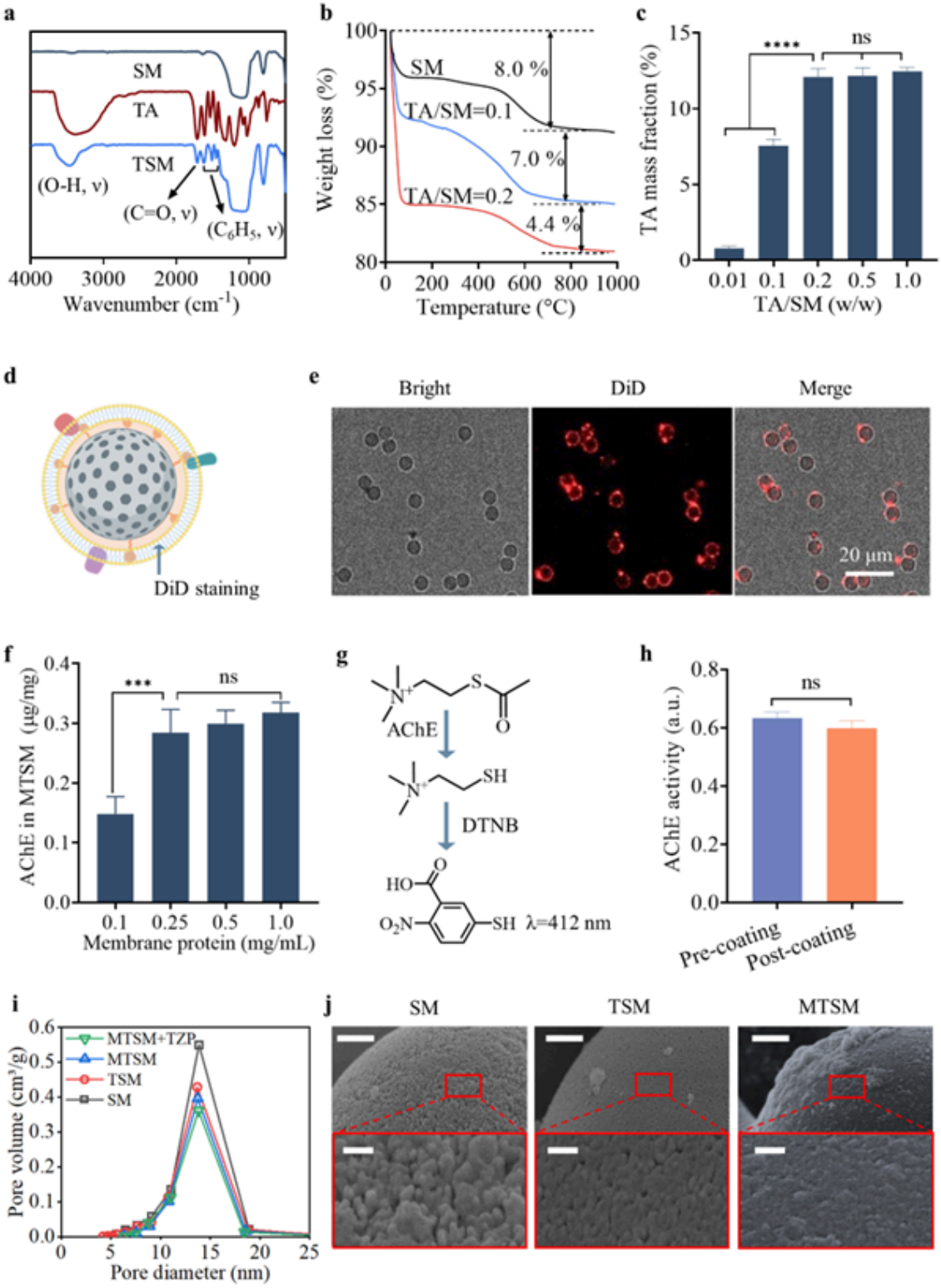

Figure 2

Characterization of locust cell membrane and tannic acid-adapted mesoporous silicon microparticles (MTSM). a, FTIR spectra of mesoporous silicon microparticles (SM), tannic acid (TA), and tannic acid coated mesoporous silicon microparticles (TSM). **b**, Thermogravimetric curves of TSM prepared at TA/SM weight ratios of 0.1 and 0.2. **c**, TA mass fraction in TSM prepared at different TA/SM weight ratios determined by bicinchoninic acid assay (BCA). **d,** Structure diagram of MTSM whose outmost layer

(locust cell membrane) stained with DiD fluorescence dye for tracking. **e**, Confocal images of MTSM inserted with DiD (red). **f**, AChE content in MTSM prepared at different amount of locust cell membrane quantified with proteins concentrations. **g**, Diagram of characterization method of AChE activity. In the presence of AChE, acetylthiocholine was degraded into thiocholine, which induced the cleavage of disulfide bonds of 5,5'-dithiobis-(2-nitrobenzoic acid) (DTNB) to form TNB with UV absorbance at 412 nm. **h**, AChE bioactivity change following the membrane coating via ultrasound quantified by measuring the catalytic activity towards acetylcholine. Statistical analysis was performed by using a two-tailed Student's t-test (ns: not significant). **i**, Pore size distribution of microparticles determined by Brunauer-Emmett-Teller (BET) method. **j**, SEM images of microparticles. The images in below row were the magnification of the rectangular region of the above row. Scale bars: 500 nm (top), 100 nm (below).

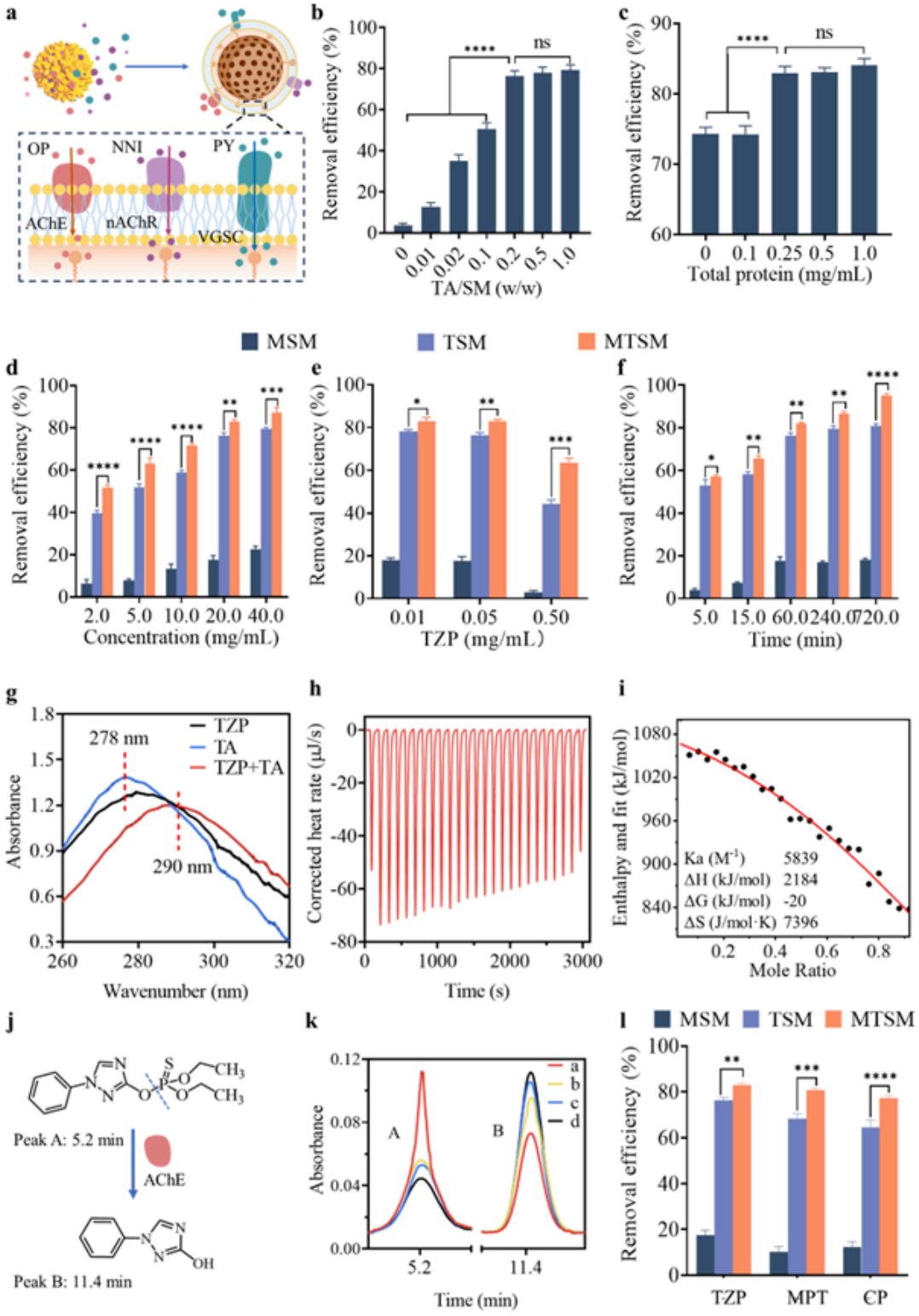

Figure 3

Removal efficiency of organophosphorus insecticides by MTSM. The treatment time was 60 min, the pH was 6.5, and the concentrations of microparticles and insecticides were 20 mg/mL and 50 μg/mL, respectively, if not otherwise mentioned. **a**, Scheme of biomimetic recognition of insecticides by MTSM. **b**, Effect of TA coating on TZP removal. **c**, Effect of locust cell membrane coating on TZP removal. **d**, Effect of microparticle concentrations on TZP removal. **e**, Effect of TZP concentrations. **f**, Effect of

incubation time. **g**, UV-vis spectra of the mixture of TA and TZP in PBS (pH=6.5). **h-i**, Isothermal titration calorimetry of TZP (0.1 mM) and TA (0.5 mM). **j**, Degradation reaction of TZP triggered by AChE. TZP and its degradation product (phenyltriazolol) could be monitored by HPLC with different elution time as illustrated. **k**, TZP and phenyltriazolol was monitored by HPLC following the co-incubation of TZP with MTSM for (**a**) 5 min, (**b**) 15 min, (**c**) 60 min and (**d**) 240 min, respectively. **l.** Removing efficiency of different OP insecticides including triazophos (TZP), methyl parathion (MPT), and Chlorpyrifos (CP) by MTSM.

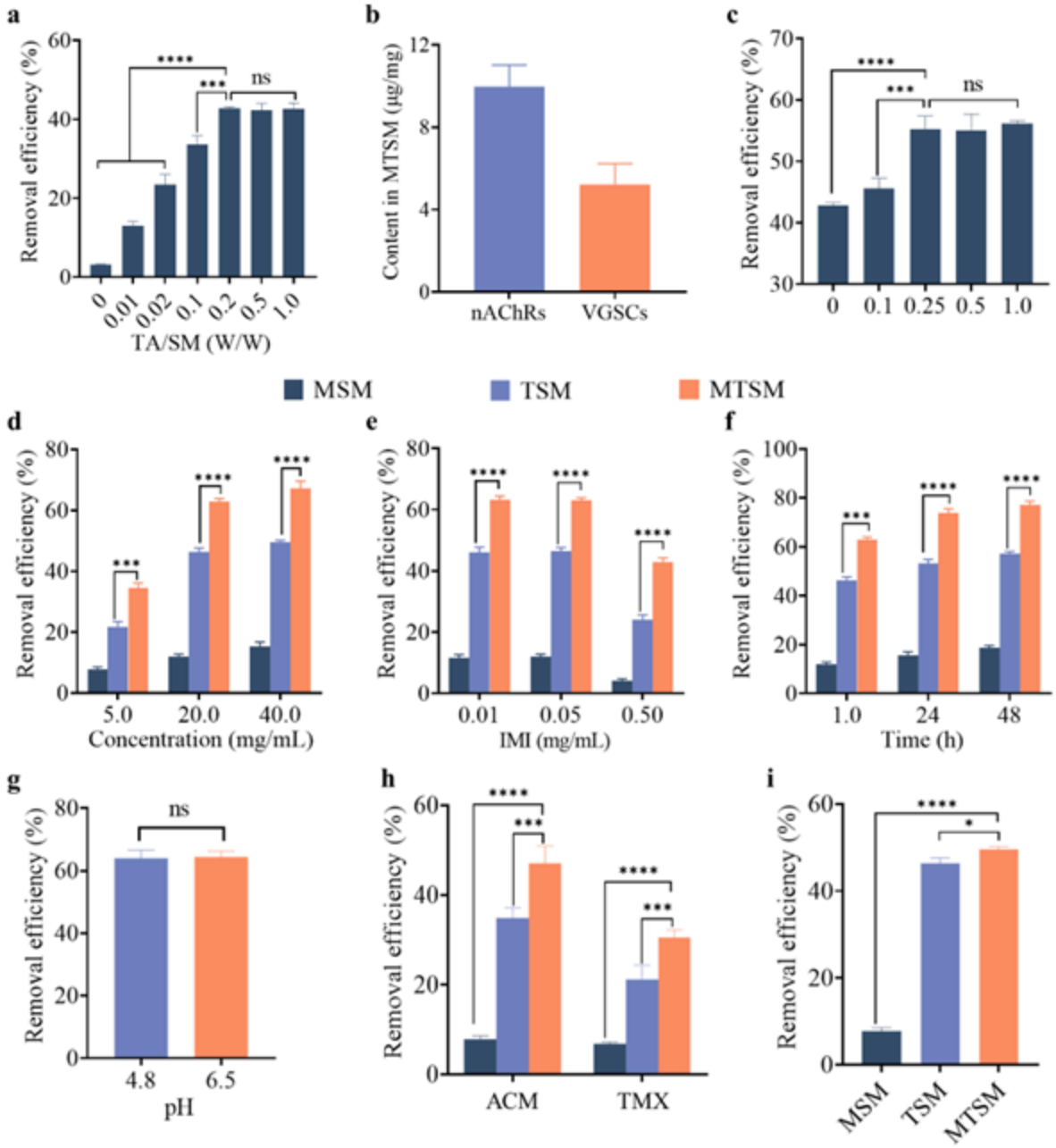

Figure 4

Removal efficiency of neonicotinoid and pyrethrin insecticides by MTSM. If not otherwise mentioned, the treatment time was 60 min, the pH was 6.5, and the concentrations of microparticles and insecticides were 20 mg/mL and 50 μg/mL, respectively. **a**, Effect of TA coating on IMI removal. **b**, nAChRs and

VGSCs content in MTSM prepared at locust cell membrane quantified with 0.25 mg/mL proteins concentrations. **c**, Effect of locust cell membrane coating on IMI removal. **d**, Effect of microparticle concentrations on IMI removal. **e**, Effect of IMI concentrations. **f**, Effect of treatment time on IMI removal. **g**, pH Effect on IMI removal efficiency of MTSM. **h**, Removal efficiency of acetamiprid and thiamethoxam. **i**, Removal efficiency of chlorpyrifos.

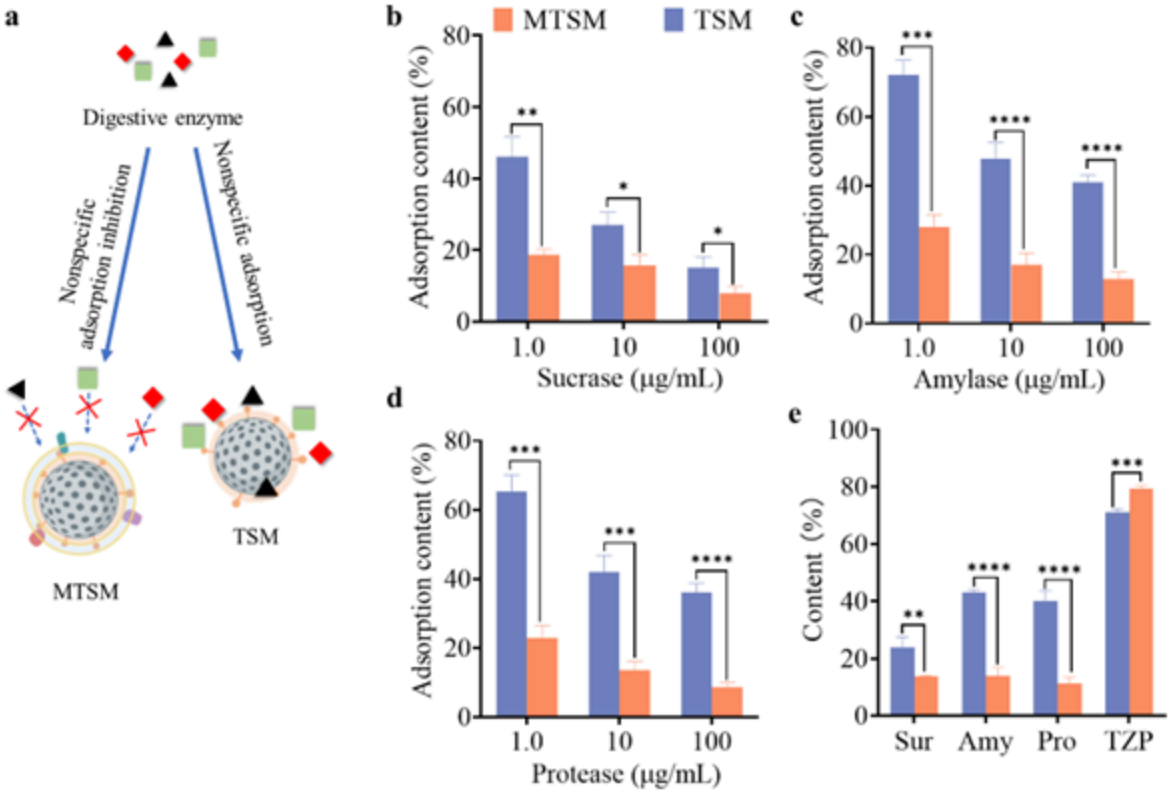

Figure 5

Inhibition of nonspecific adsorption by MTSM. a, Schematic illustration of nonspecific adsorption of different digestive enzymes. **b-d**, Inhibition of nonspecific adsorption of digestive enzymes **b**, sucrase; **c**, amylase; **d**, protease existing in gastrointestinal (GI) system of pollinators. **e**, Selective removal of TZP under the environment of GI enzymes.

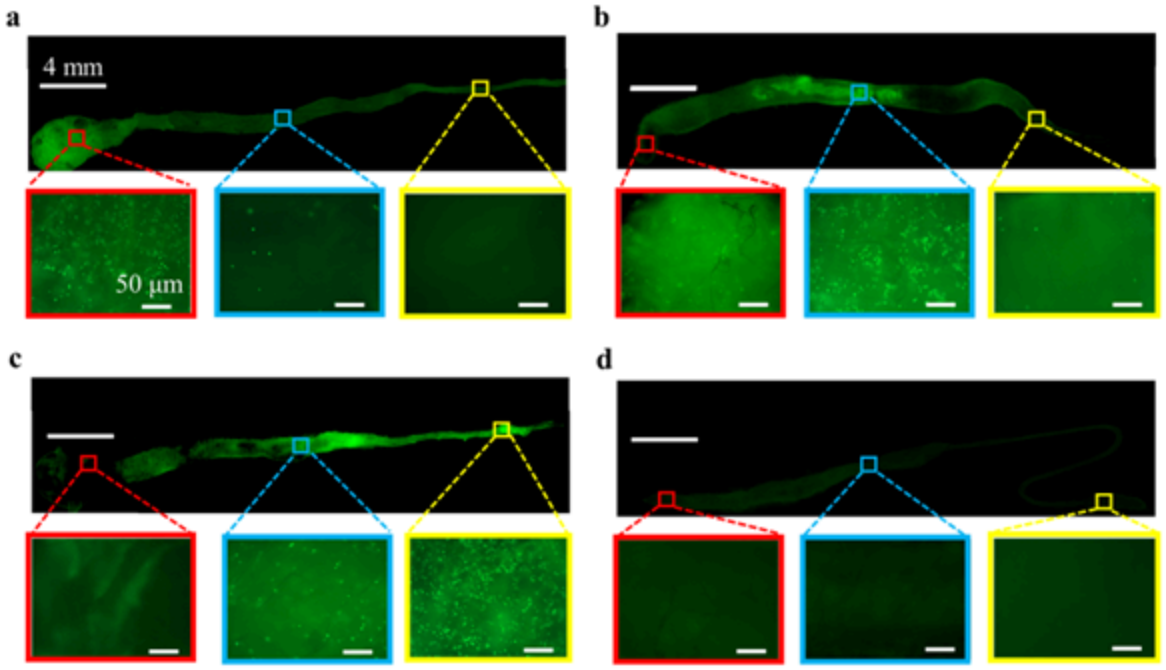

Figure 6

In vivo gastrointestinal distribution of MTSM. FITC-labeled MTSM in the gastrointestinal tract of bumblebees was tracked using fluorescent imaging within 0 h (**a**), 4 h (**b**), 12 h (**c**), 48 h (**d**). Red rectangle: crop stomach or proventriculus; blue rectangle: midgut; yellow rectangle: hindgut.

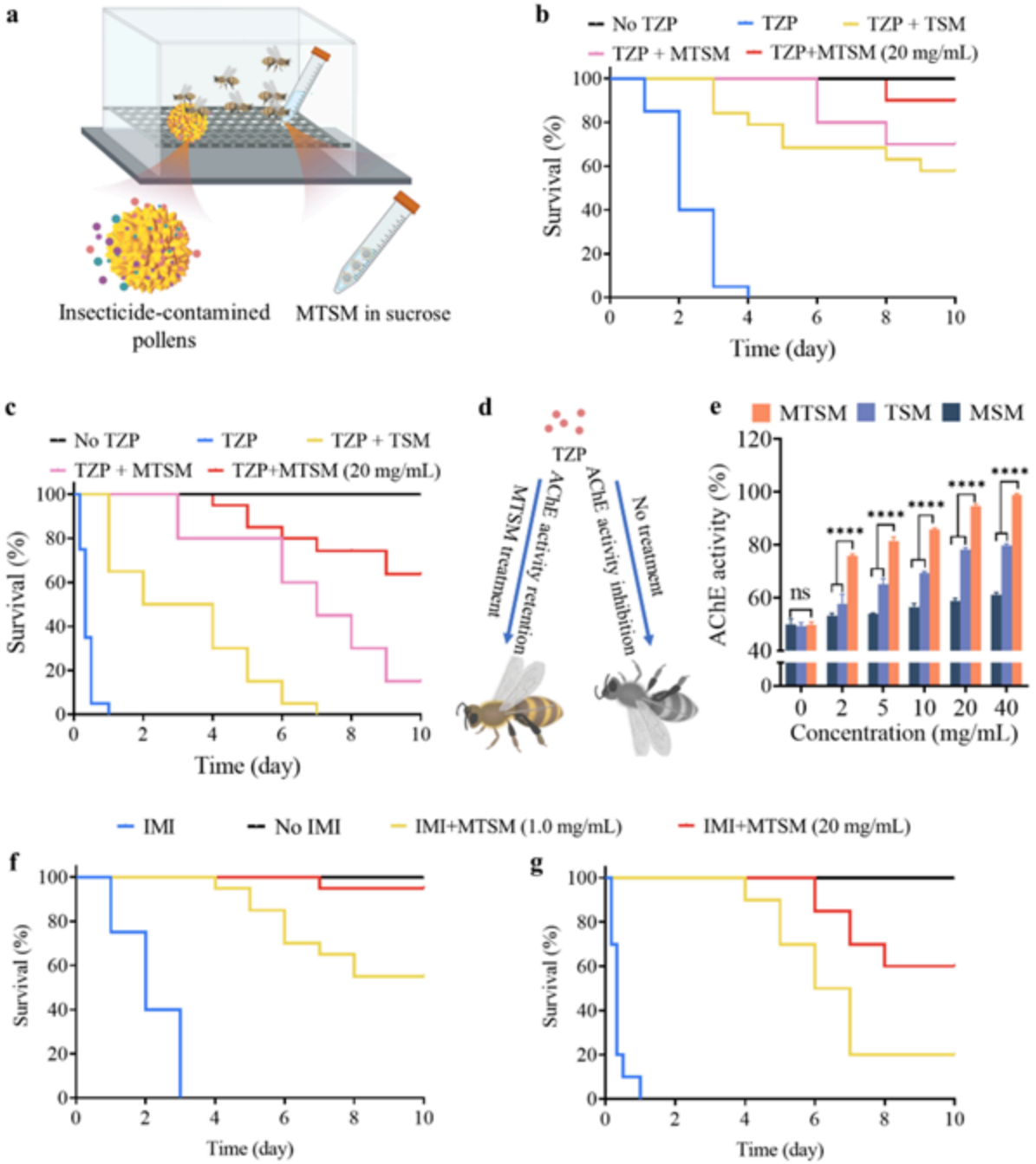

Figure 7

In vivo detoxification of insecticides in bumblebee using MTSM. a, Schematic illustration of in vivo detoxification. **b**, Survival rate of bumblebees treated with TZP (60 μg TZP/g in pollen) and microparticles. **c**, Survival rate of bumblebees treated with TZP (120 μg TZP/g in pollen) and microparticles. **d**, Schematic illustration of AChE activity protection in bumblebees by MTSM. **e**, AChE activity of bumblebee cell membrane following the treatment with the supernatant of the mixture of TZP (20 mg/mL) microparticles at different concentrations. **f**, Survival rate of bumblebees treated with IMI (5 μg IMI/g in pollen). **g**, Survival rate of bumblebees treated with IMI (15 μg IMI/g in pollen).

Supplementary Files

This is a list of supplementary files associated with this preprint. Click to download.

- SI2024.docx